Journal of Fundamental and Applied Sciences

ISSN 1112-9867

Available online at http://www.jfas.info

Research Article

GEOPHYSICAL ASSESSMENT OF GROUNDWATER CONTAMINATIONS FROM LEACHATE INTRUSION IN AMOYO DUMPSITE

S. Olatunji, A. O. Fauzan*

Department of Geophysics, University of Ilorin, PMB 1515, Ilorin, Nigeria

Received: 10 August 2021 / Accepted: 19 November 2021 / Published online: 01 January 2022

ABSTRACT

The work aims to map the extent of leachate intrusion in near-surface rocks around a reclaimed dumpsite (40 years old) in Amoyo town. Sixteen very low-frequency electromagnetic (VLF - EM) profiles were distributed in the four cardinal directions around the site. Twenty-nine (29) points were sounded, using Schlumberger approach, at all identified VLF anomalous points. The analyzed VLF-EM data revealed the presence of conductive pollutants (leachate plumes) at the subsurface. The geo-electric sections generated from the processed VES data supported the VLF-EM results. It is concluded that (i) leachate is still present in the rock formation of the reclaimed dumpsite several years after the abandonment and excavation of the waste materials (ii) the shallow aquifer is at risk of contamination (iii) the low resistivity of the basement rocks signified presence of leachates.

Keywords: Dumpsite; Leachate; Groundwater; VLF-EM; Electrical sounding

Author Correspondence, e-mail: akomolafefauzan@gmail.com

doi: http://dx.doi.org/10.4314/jfas.v14i1.10

1. INTRODUCTION

The quality necessary for groundwater supply is majorly controlled by its essence [1]. Drinking, bathing, cooking, and general sanitation such as laundry, closet flushing, and other household chores are the primary resolutions for which water is nationally important, while it is primarily used for irrigation and livestock among other agricultural purposes [2].

Ramakrishnaiah [3] stated that the population explosion, combined with the expansion of industry, has increased the development of a variety of wastes, ranging from municipal to industrial, all of which harm human health through groundwater quality. The quantity and quality of recharged water, produced waste, sewage treatment, and geochemical processes in the near-surface all regulate groundwater quality [4].

Groundwater pollution is a thought-provoking phenomenon in Nigeria because most cities face solid waste management issues such as insufficient waste disposal equipment, and waste disposal site siting within residential areas without consideration for local geology and hydrogeology, among other conditions [5]. The conditions that are stated above influenced the contamination of the nearby groundwater resources. Open dumping mode of waste disposal can harm adjacent water sources if the leachate originated from decomposed solid waste infiltrates and contaminates the water table [5]. A leachate is any liquid that, in the course of passing through matter, extracts *soluble* solids, or any other component of the material through which it has passed. The structure of the waste constituents, the presence of moisture, and the local temperature conditions all influence the characteristics and dimensions of leachate formed in a dumpsite [6]. According to MacDonald [7]; dumpsite leachate is considered the worst recognized source of shallow groundwater aquifer contamination.

Electric current conducts poorly through rocks and soil. When the rocks and soils are infiltrated by leachate or polluted water containing a large number of dissolved ions, the conductivity of the rocks will increase from low to moderate to unusually high [8]. Electrical resistivity and electromagnetic techniques have been developed as very suitable surface geophysical methods due to the conductive nature of most pollutants [9-12]. Related techniques were used in the past for landfill characterization and delineation [13-18] and also in waste disposal site investigation.

Geophysical electrical methods such as Very Low-Frequency Electromagnetic (VLF-EM) and Vertical Electrical Sounding (VES) are used for studying pollution. The techniques have been used to evaluate dumpsites and landfills, chart leachate flows around dumpsites, examine groundwater pollution, and classify geo-electric layers with great success. The easiest electromagnetic (EM) technique for identifying shallow subsurface conducting structure is the very-low-frequency (VLF) method. The method is ideal for depicting conducting structures up to 200 m depth in extremely resistive terrain since it uses signals emitted from worldwide transmitters located in coastal areas in the 15–25 kHz frequency band. This is a geophysical ground-penetrating system that uses Very Low-Frequency signals in the 5–30 kHz range, which are widely used for submarine and military communication. The electromagnetic

radiation emitted in the low-frequency width of (15–25 kHz) by powerful radio transmitters used in long-range communications and navigational systems is used by VLF- techniques. Although the conductivity of soils and rocks is generally low to moderate, leachate-contaminated rocks and soils are expected to have strong positive Very Low-Frequency Electromagnetic signatures [6].

Electrical resistivity techniques have equally proven to be resourceful for this form of environmental research. This is because the ionic concentration of leachate is typically much higher than that of groundwater, resulting in a significant contrast in electrical properties as the leachate reaches the aquifer. The method would recognize these areas as an anomaly, allowing the leachate plume to be identified. The basic rule is that the further apart the current electrodes are, the greater the penetration depth [19], [20]. Although moderate resistivity values are expected in freshwater-saturated rock units, very low resistivity values indicate the presence of dissolved ions, likely from leachates [21]. The aim of this study is to map in detail the leachate pollution in soil and rock units around the reclaimed dumpsite to know if the overburden in the study area was able to prevent leachate flow to the adjoining areas. In addition to mapping the contaminant leachate, the study seeks to: (i) investigate the vertical scale of leachate migration, to determine the depth to the areas “protected aquifer” (ii) determine the fracture distribution (iii) determine the number of geo-electric layers (iv) estimate depth to fresh basement rock (v) determine overburden thickness to the aquifer (vi) correlate between the geochemical and geophysical data on aquifer characteristics.

1.1 The Study Area

The study area (Figure 1) is an abandoned open dumpsite at a town called Amoyo along Ilorin-Ajase Road, Ilorin, Kwara State, Nigeria. It is about 40 years old (personal communication with a local, 2021), the area is located within the basement complex of southwestern Nigeria. It lies between longitudes 4° 38′ 45.82″ E and 4° 40′ 13.46″ E and latitudes 8° 26′ 52.94″ N and 8° 24′ 13.53″ N, covering approximately 13.28 km^2. Amoyo is located on a depression's crest, with a well-dissected landscape covered in laterites. Some residential houses and farmland surround the landfill. The dumpsite was stopped from operation as a result of the cholera outbreak in the region which led to the deaths. The dumpsite has been converted to a residential area. Field study and geophysical mapping took place in the year 2021, during the dry season. The study area is generally accessible through un-tarred roads as well as footpaths. In some parts, however, accessibility is easier during the dry seasons.

As per the climate, topography and drainage system, the area is strategically situated between Nigeria's heavily populated South-Western region and the sparsely populated middle belt [22]. The climate in the research area is humid tropical, with rainy and dry seasons. The rainy season in the area starts around the end of March and lasts until the end of October. The annual average rainfall is 11.5 mm, which is reasonably uniformly distributed [23]. The wettest months are June through early August, with a brief drought in August and September. In October, the dry season starts and lasts until late February or early March. Due to harmattan, December and January are usually cold months [23]. The study area's drainage scheme follows a dendritic pattern. The Asa River runs through a fairly wide valley and divides the study area into two sections, the eastern and western halves.

1.2 Concise Geology of the study area

The region (Figure 2) is geologically part of the migmatite-gneiss-quartzite zone of the basement complex of South Western Nigeria, and it is within the 600-150-million-year Pan African reactivation zone [24]. Migmatite, quartzite, and granite are the most common rock types found in the study region. These rock types have weathered to form the study area's soil cover. Due to the tropical climatic conditions, surficial materials are characterized by comparatively heavily weathered soil profiles in low-lying areas. Lateritic soils make up a higher part of the topsoil. Lateritic soils are typically formed by the weathering of parent sedimentary (limestone), metamorphic (schists, gneisses, migmatite), and igneous (granites, basalts, gabbros, peridotites) rocks. Lateritic soils are formed as a result of the weathering of metamorphic (gneisses, migmatite) and igneous (granite) rocks, which leave the more insoluble ions, mostly iron and aluminum. As a result, lateritic soils are high in aluminum and iron, and they are frequently associated with tropical environments, especially in Nigeria's basement complex terrains.

Water table depth, contaminant concentrations, and geologic strata permeability; Water can become partly diluted when it percolates downwards into the soil if the water table is shallow (far below the ground surface). Contaminants can penetrate groundwater directly without being treated by the soil if the water table is shallow (close to the ground surface). Groundwater contamination would be more likely if leachate has a high concentration of toxins. Further, leachate can easily percolate through extremely permeable geologic strata with no filtration along the way. Strata made up of comparatively impermeable materials including silt and clay serve as a natural barrier to leachate, preventing it from percolating downward.

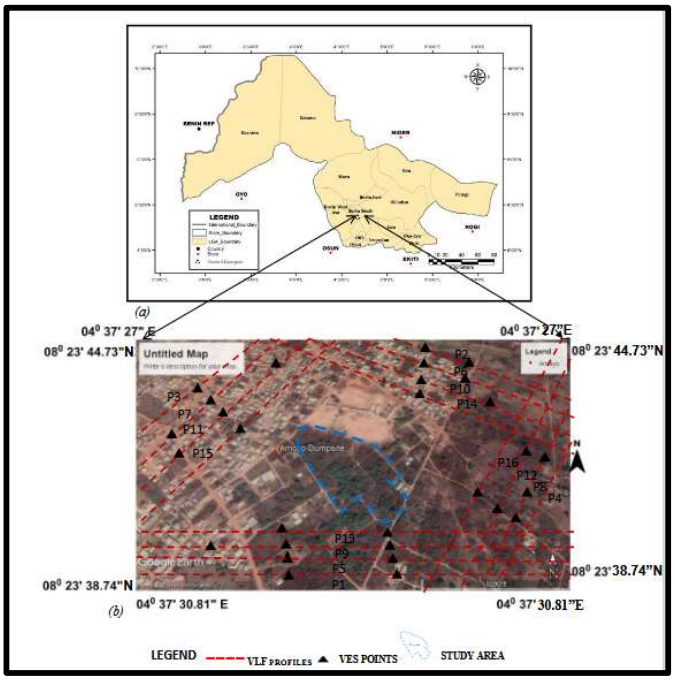

Fig.1. Map of Kwara state showing the study area (b) Site map of the study area showing VLF profiles and VES stations

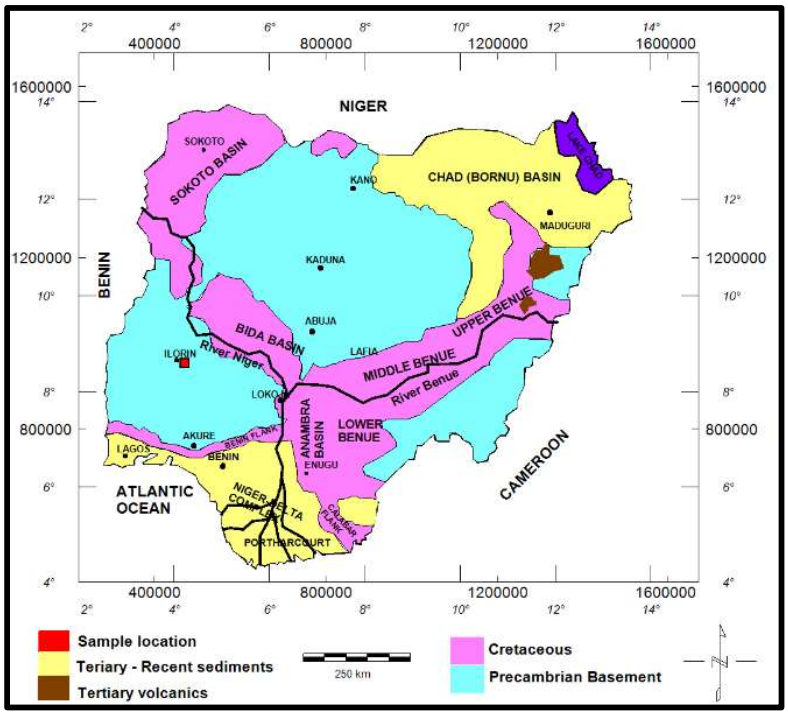

Fig.2. Geological map of Nigeria showing the sample location [25]

2. MATERIAL AND METHODS

2.1 VLF data acquisition and processing

Inductive prospecting techniques based on the VLF-EM system are used to map shallow subsurface structural features under which primary electromagnetic (EM) wave causes current to pass [26], [27], [28]. A ground trotting geophysical tool for mapping 2D/3D conductivity distribution in geological systems at the subsurface is a very low-frequency electromagnetic survey. Worldwide radio signal transmitters designed specifically for electronic and submarine communication typically have the primary electromagnetic field. The transmitting station's frequencies normally vary from 15 to 30 kHz. Low-frequency spectrum transmitters are chosen for this VLF-EM survey to achieve deep penetration and reduce electromagnetic signal attenuation. Around the globe, VLF-EM transmitter stations can be found. They are mainly used to relay radio signals at frequencies ranging from 10 to 30 kHz for submarine communication. The selection of a 15.8 kHz transmitter that generates a primary electromagnetic field that is, north-south oriented and roughly parallel to the strike of the rocks in the research region was the first step in the VLF-EM field measurements for this study. The secondary electromagnetic field, which is shifted in phase to the primary electromagnetic field, was generated by conductive bodies in the study area. The vertical (H_Z) and horizontal (H_X) components of the secondary electromagnetic field are measured every 5 m with *WADI* (ABEM) VLF equipment along with the defined profiles. The field's horizontal and vertical components are connected by the scalar B, tipper, which is defined as:

$$B = \frac{H_z}{Hx} \quad (1)$$

The time difference between the primary and secondary electromagnetic fields is denoted by **B** [29]. **B** is made up of both real and imaginary components. For geophysical interpretation, only the actual component is used. The hypothetical component is often tainted by noise and erroneous evidence. To prevent measurement errors, the transmitting station was not modified during the field survey. There were four profiles on either side of the dumpsite core (north, south, west, and east) as depicted in Figure 1. The profiles were roughly N-S and E-W in orientation. Since buildings in the region block the VLF profile duration, the profile length ranges from 200 m to 180 m based on room availability. The real component of the data is filtered using Fraiser's procedure (1966). The filtered actual portion of the data is used to calculate the current density pseudo-section for each VLF profile using the method of Karous and Hjelt [26]. The KHFILT inversion program is used to calculate and plot the current density pseudo-section [30]. Skin depth normalization is used in the inversion to

compensate for the influence of attenuation with depth. A total of 16 VLF profiles were covered (Figure 1), forming four-square grids around the dumpsite at 20 m inter-profile spacing and 5 m interstation spacing. Profile 1 is 20 m south of the dumpsite center. Profiles 5, 9, and 13 are separated by 20m inter-profile spacing from profile 1. Profile 2 is 20m north of the dumpsite center. Profile 6, 10, and 14 are separated by 20 m inter-profile spacing from profile 2. Profile 3 is 20 m west of the dumpsite center. Profile 7, 11, and 15 are separated by 20 m inter-profile spacing from profile 3. Profile 4 is 20 m east of the dumpsite center. Profile 8, 12, and 16 are separated by 20 m inter-profile spacing from profile 4.

2.2 Electrical resistivity data acquisition and processing

A total of 29 1D VES points were performed at pre-determined locations as shown in Figures 1. VES points were located at all VLF anomalous points, having interpreted VLF data. The VES survey aims to investigate certain conductivity structures seen in the VLF data, identify the geo-electric layers equivalent to geologic strata, and estimate the depth to fresh basement rocks. The basic intention was to detect possible leachate intrusions. A code written in Matlab was used to reduce noise and spurious data in VES data. Four data filtering systems are used in the code. To obtain the geo-electric parameters of each sheet, the curves are first manually interpreted using master curves [31], [32]. The filtered data was then fed into an IPI2WIN program [33] for further analysis. The maximum and minimum layer numbers for the inversion scheme are determined by the number of layers derived from manual interpretation. For example, where 3 layers are interpreted for a VES curve, a minimum of two and a maximum of four layers are set for the VES inversion scheme. The field data curve and theoretical curve converge after a few iterations.

The 2-dimensional view of the geo-electric parameters (resistivity and thickness) obtained from the inversion of the electrical resistivity sounding data was used to adjudge the aquiferous or non-aquiferous layers and reliable geological deductions. The geo-electric sections of the various VES stations in the study area were created to indicate the various geo-electric layers, their thicknesses within the depths penetrated with their characteristic's resistivity values, and probable geo-electric connotations. Finally, the geophysical results were compared with the geochemical results of Musa and Sikemi [34], for correlation and confirmations of results.

3. RESULTS AND DISCUSSIONS

3.1 VLF – EM results

The Karous-Hjelt current density data plots were employed for the VLF-EM data interpretation to detect the leachate flow and to map its spatial distribution as shown from Figure (3 – 18). The cross-section of the apparent current density of profile 1 (Fig. 3a) reveals the presence of anomalies between 35 – 45 m (top location, 40 m). Figure 3b shows the Fraser filtering Plot for profile 1 In-phase VLF response generated using the *KH-Filter* Geophysical software program from which figure 3c was produced. The inversion of profile 1 (Fig. 3c) demonstrates the presence of low resistivity values below 15 Ωm which extend to 20 m depth; this coincides with the landfill structure boundaries between 35 m and 45 m and from 150 m to 160 m. The areas that are marked by arrows are the points that are sounded by VES techniques. They were meant to investigate the contrasting conductivity structures observed in the VLF-EM results at the two points.

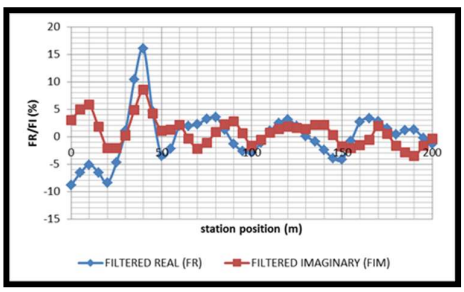

a. Filtered real and filtered imaginary

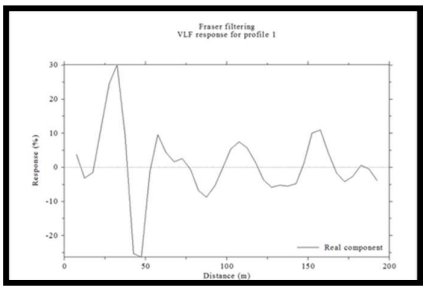

b. Fraser Filter In-phase plot

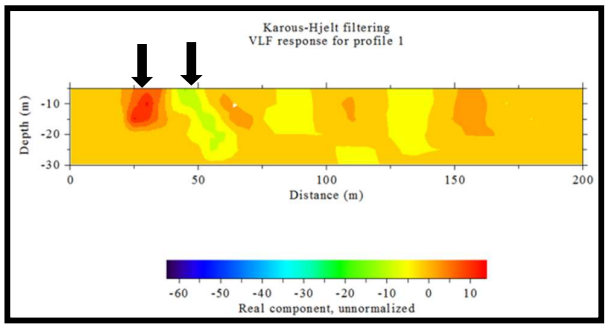

c. 2D cross-section equivalence of VLF response (P1)

Fig.3. VLF-EM Responses for profile 1

The cross-section of the apparent current density of profile 5 (Fig. 4a) reveals the presence of anomalies between 20 – 35 m (top location, 30 m), 85–110 m (top location, 100 m), and 180 - 190m (top location, 185 m). Figure 4b shows the Fraser filtering Plot for profile 5 In-phases VLF responses generated using the *KH-Filter* Geophysical software program from which

figure 4c was produced. The inversion of profile 5 (Fig. 4c) demonstrates the presence of low resistivity values below 15 Ωm which extend to 30 m depth; this coincides with the landfill structure boundaries between 70 m and 110 m and from 170 m- 180 m. The cross-section of the apparent current density of profile 9 (Fig. 5a) reveals the presence of anomalies between 20 – 40 m (top location, 25 m), 50 – 65 m (top location, 60 m), and 125 – 140 m (top location, 135 m). Figure 5b shows the Fraser filtering Plot for profile 9 In-phases VLF responses generated using the *KH-Filter* Geophysical software program from which figure 5c was produced. The inversion of profile 5 (Fig. 5c) demonstrates the presence of low resistivity values below 15 Ωm which extend to 15 m depth; this coincides with the landfill structure boundaries between 10 m and 25 m, 40 m and 50m and 75 m and 120 m. The areas that are marked by arrows are the points that are sounded by VES techniques. They were meant to investigate the contrasting conductivity structures observed in the VLF-EM results at the points.

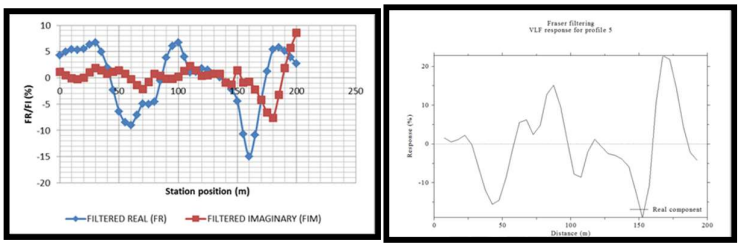

a. Filtered real and filtered imaginary *b. Fraser Filter In-phase plot*

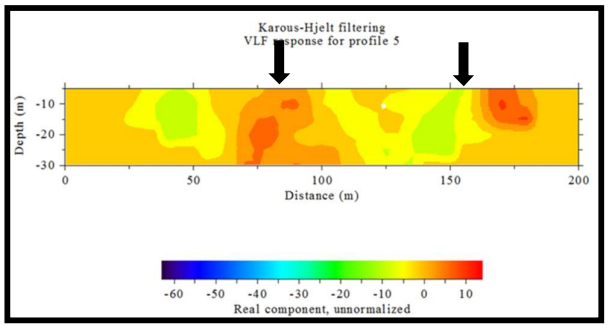

c. 2D cross-section equivalence of VLF response (P5)

Fig.4. VLF-EM Responses for profile 5

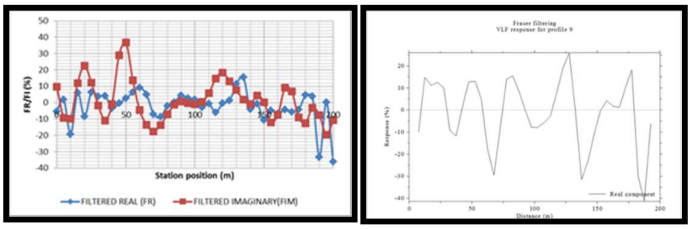

a. Filtered real and filtered imaginary *b. Fraser Filter In-phase plots*

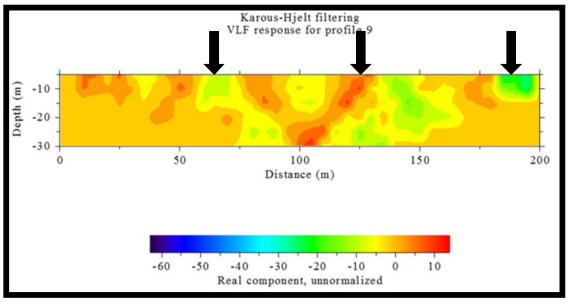

c. 2D cross-section equivalence of VLF response (P9)

Fig.5. VLF-EM Responses for profile 9

Similarly, the cross-section of the apparent current density of profile 13 (Fig. 6a) reveals the presence of anomalies between 15 – 25 m (top location, 20 m), 40 – 50 m (top location, 45 m), and 90 – 100 m (top location, 95 m). Figure 6b shows the Fraser filtering Plot for profile 13 In-phases VLF responses generated using the *KH-Filter* Geophysical software program from which figure 6c was produced. The inversion of the profile 13 (Fig. 6c) demonstrates the presence of low resistivity values below 15Ωm which extend to 15 m depth; this coincides with the landfill structure boundaries between 10 m and 20 m and between 35 - 50 m, 130 m, and 110 m and 125 m, and 160 m – 175 m. The cross-section of the apparent current density of profile 2 (Fig. 7a) reveals the presence of anomalies between 5 – 25 m (top location, 15 m), 75 – 85 m (top location, 80 m), and 155 – 180 m (top location, 170 m). Figure 7b shows the Fraser filtering Plot for profile 2 In-phases VLF responses generated using the *KH-Filter* Geophysical software program from which figure 7c was produced. The inversion of profile 2 (Fig. 7c) demonstrates the presence of low resistivity values below 10 Ωm which extend to 15 m depth; this coincides with the landfill structure boundaries between 75 m, and 150 m and 165 m. The cross-section of the apparent current density of profile 6 (Fig. 8a) reveals the presence of anomalies between 75 – 95 m (top location, 90 m), and 140 – 160 m (top location, 150 m). Figure 8b shows the Fraser filtering Plot for profile 6 In-phases VLF responses generated using the *KH-Filter* Geophysical software program from which figure 8c was produced. The inversion of profile 6 (Fig. 8c) demonstrates the presence of low resistivity

values below 15 Ωm which extend to 30 m depth; this coincides with the landfill structure boundaries between 55 m and 75 m, and 120 m and 130 m. The cross-section of the apparent current density of profile 10 (Fig. 9a) reveals the presence of anomalies between 45 – 55 m (top location, 50 m), and 125 – 140 m (top location, 135 m). Figure 9b shows the Fraser filtering Plot for profile 10 In-phases VLF responses generated using the *KH-Filter* Geophysical software program from which figure 9c was produced. The inversion of profile 10 (Fig. 9c) demonstrates the presence of low resistivity values below 15Ωm which extend to 30 m depth; this coincides with the landfill structure boundaries between 10 m and 30 m, and 75 m and 125 m. The cross-section of the apparent current density of profile 14 (Fig. 10a) reveals the presence of anomalies between 45 – 55 m (top location, 50 m), 105 – 115 m (top location, 110 m), and 160 m – 180 m (top location, 170 m). Figure 10b shows the Fraser filtering Plot for profile 14 In-phases VLF responses generated using the *KH-Filter* Geophysical software program from which figure 10c was produced. The inversion of profile 14 (Fig. 10c) demonstrates the presence of low resistivity values below 15Ωm which extend to 30 m depth; this coincides with the landfill structure boundaries between 30 m and 60 m and from 75 m to 125 m. The area that is marked by arrow is the point that is sounded by VES method. They were meant to investigate the contrasting conductivity structures observed in the VLF-EM results at the two points.

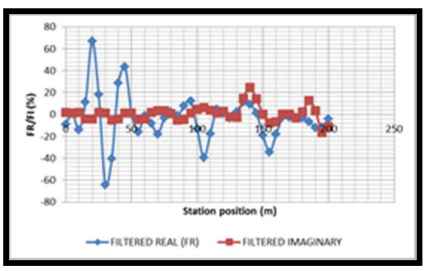

a. Filtered real and filtered imaginary

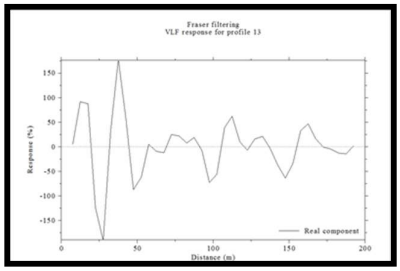

b. Fraser Filter In-phase plot

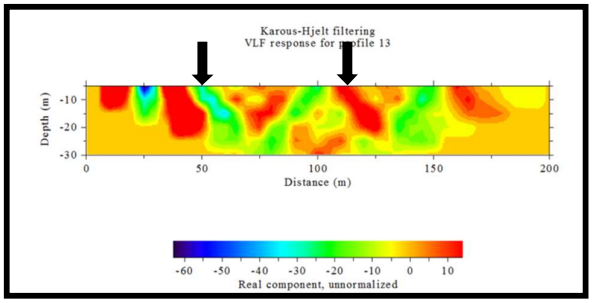

c. 2D cross-section equivalence of VLF response (P13)

Fig.6. VLF-EM Responses for profile 13

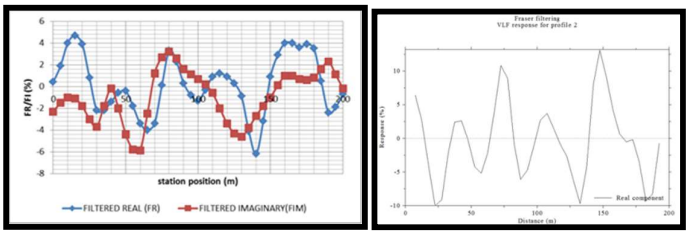

a. Filtered real and filtered imaginary *b. Fraser Filter In-phase plot*

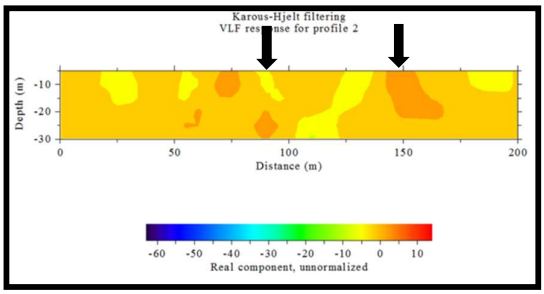

c. 2D cross-section equivalence of VLF response (P2)

Fig.7. VLF-EM Responses for profile 2

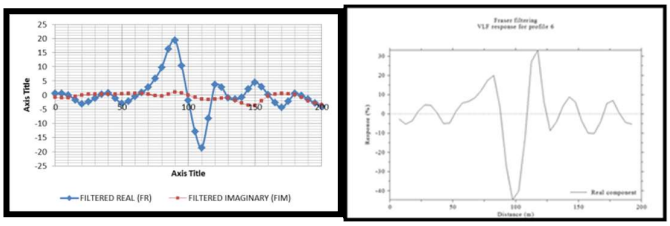

a. Filtered real and filtered imaginary *b. Fraser Filter In-phase plot*

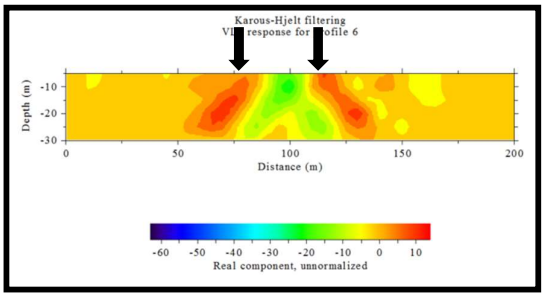

c. 2D cross-section equivalence of VLF response (P6)

Fig.8 VLF-EM Responses for profile 6

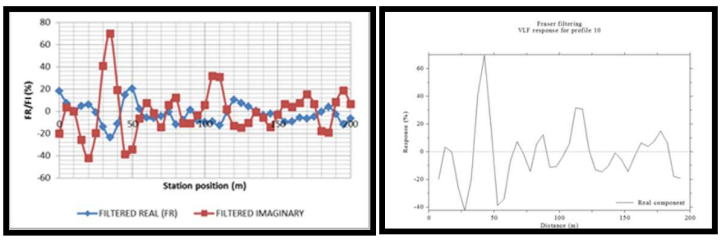

a. Filtered real and filtered imaginary *b. Fraser Filter In-phase plot*

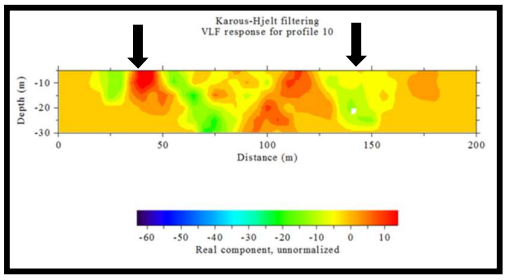

c. 2D cross-section equivalence of VLF response (P10)

Fig.9. VLF-EM Responses for profile 10

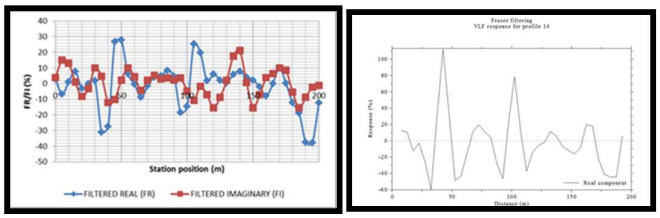

a. Filtered real and filtered imaginary *b. Fraser Filter In-phase plot*

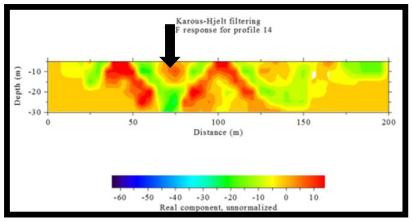

c. 2D cross-section equivalence of VLF response (P14)

Fig.10. VLF-EM Responses for profile 14

The cross-section of the apparent current density of profile 3 (Fig. 11a) reveals the presence of anomalies between 30 – 50 m (top location, 40 m), 65 – 80 m (top location, 70 m), 100 m – 115 m (top location, 110 m) and 150 m – 190 m (top location, 170 m). Figure 11b shows the Fraser filtering Plot for profile 3 In-phases VLF responses generated using KH-Filter Geophysical software program from which figure 11c was produced. The inversion of profile 3 (Fig. 11c) demonstrates the presence of low resistivity values below 15Ωm which extend to 15 m depth; this coincides with the landfill structure boundaries between 20 - 28 m and 75 - 85 m. The cross-section of the apparent current density of profile (Fig. 12a) reveals the presence of anomalies between 85 – 100 m (top location, 90 m), and 180 – 200 m (top location, 190 m). Figure 12b shows the Fraser filtering Plot for profile 7 In-phases VLF responses generated using the *KH-Filter* Geophysical software program from which figure 12c was produced. The inversion of profile 7 (Fig. 12c) demonstrates the presence of low resistivity values below 15Ωm which extend to 30 m depth; this coincides with the landfill structure boundaries between 55 m and 110 m and from 160 m to 170 m.

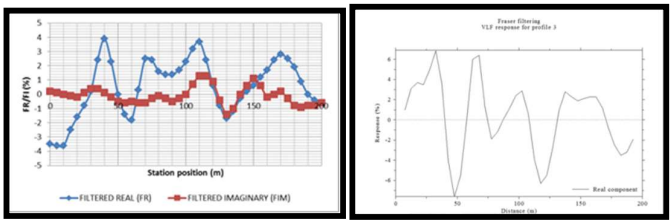

a. Filtered real and filtered imaginary *b. Fraser Filter In-phase plot*

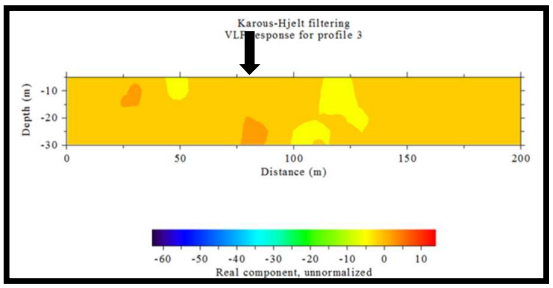

C. 2D cross-section equivalence of VLF response (P3)

Fig.11. VLF-EM Responses for profile 3

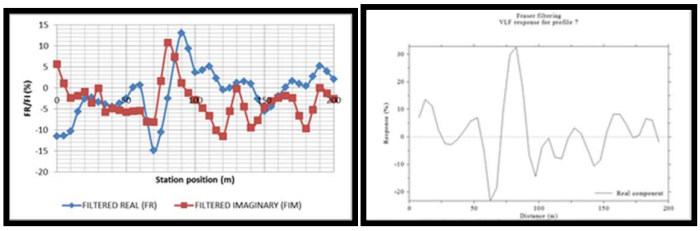

a. Filtered real and filtered imaginary *b. Fraser Filter In-phase plot*

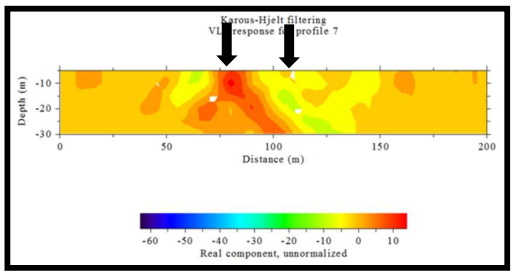

c. 2D cross-section equivalence of VLF response (P7)

Fig.12. VLF-EM Responses for profile 7

The cross-section of the apparent current density of profile 11 (Fig. 13a) reveals the presence of anomalies between 20 – 35 m (top location, 30 m), 60 – 75 m (top location, 65 m), 150 m – 170 m (top location, 165 m), and 180 m – 190 m (top location, 185 m). Figure 13b shows the Fraser filtering Plot for profile 11 In-phases VLF responses generated using the *KH-Filter* Geophysical software program from which figure 13c was produced. The inversion of profile 11 (Fig. 13c) demonstrates the presence of low resistivity values below 15 Ωm which extend

to 30 m depth; this coincides with the landfill structure boundaries between 50 m, and 100m, and 140 m to 160 m. The cross-section of the apparent current density of profile 15 (Fig. 14a) reveals the presence of anomalies between 30 – 45 m (top location, 35 m), 50 – 70 m (top location, 65 m), and 140 m – 145 m (top location, 140 m). Figure 14b shows the Fraser filtering Plot for profile 15 In-phases VLF responses generated using the *KH-Filter* Geophysical software program from which figure 14c was produced. The inversion of the profile 15 (Fig. 14c) demonstrates the presence of low resistivity values below 15 Ωm which extend to 10 m depth; this coincides with the landfill structure boundaries between 10 m to 30 m and from 40 m and 60 m, 100m and 150 m.

The cross-section of the apparent current density of profile 4 (Fig. 15a) reveals the presence of anomalies between 30 – 50 m (top location, 40 m), and 130 – 150 m (top location, 140 m). Figure 15b shows the Fraser filtering Plot for profile 4 In-phases VLF responses generated using the *KH-Filter* Geophysical software program from which figure 15c was produced. The inversion of profile 4 (Fig. 15c) demonstrates no point with low resistivity values. Except for the presence of a high resistive structure with resistivity values below -5Ωm which extend to 30 m depth around 130 and 160 m, no points were sounded in this profile. The cross-section of the apparent current density of profile 8 (Fig. 16a) reveals the presence of anomalies between 9 m – 13 m (top location, 10 m), 90 – 98 m (top location, 95 m), 100 m – 110 m (top location, 105 m), and 130 m – 150 m (top location, 140 m). Figure 16b shows the Fraser filtering Plot for profile 8 In-phases VLF responses generated using the *KH-Filter* Geophysical software program from which figure 16c was produced. The inversion of profile 8 (Fig. 16c) demonstrates the presence of low resistivity values below 15Ωm which extend to 30 m depth; this coincides with the landfill structure boundaries between 25 m to 50 m and from 80m to 100m. The areas that are marked by arrows are the point that is sounded by VES techniques. They were meant to investigate the contrasting conductivity structures observed in the VLF-EM results at the two points.

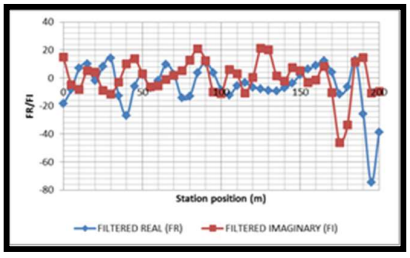

a. Filtered real and filtered imaginary

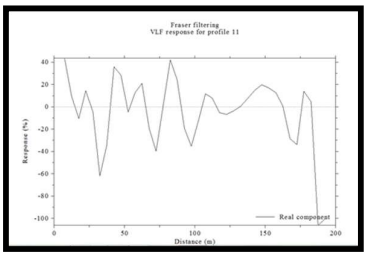

b. Fraser Filter In-phase plot

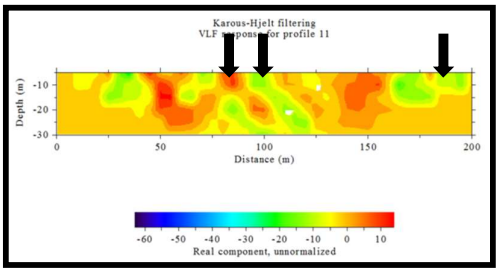

c. 2D cross-section equivalence of VLF response (P11)

Fig.13. VLF-EM Responses for profile 11

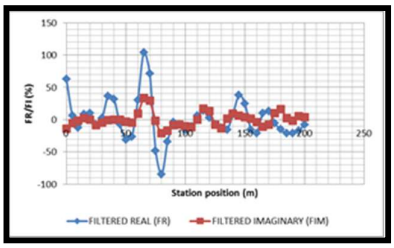

a. Filtered real and filtered imaginary

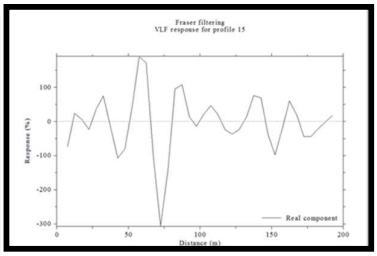

b. Fraser Filter In-phase plot

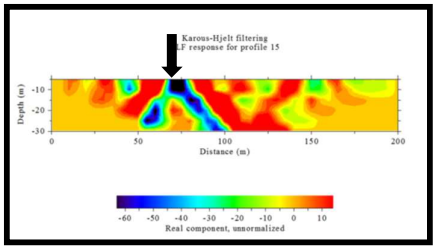

c. 2D cross-section equivalence of VLF response (P15)

Fig.14. VLF-EM Responses for profile 15

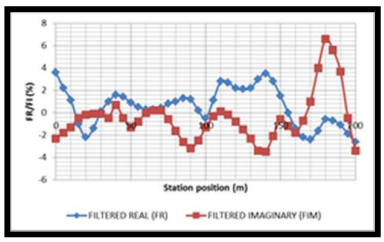

a. Filtered real and filtered imaginary

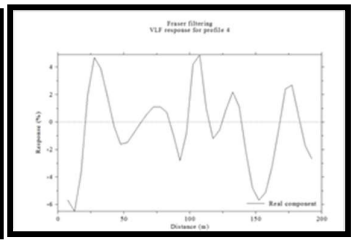

b. Fraser Filter In-phase plot

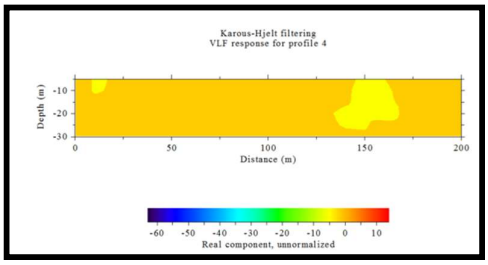

c. 2D cross-section equivalence of VLF response (P4)

Fig.15. VLF-EM Responses for profile 4

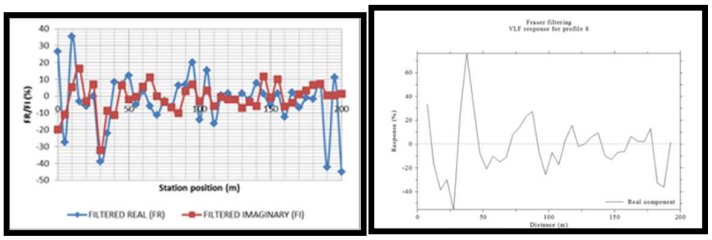

a. Filtered real and filtered imaginary *b. Fraser Filter In-phase plot*

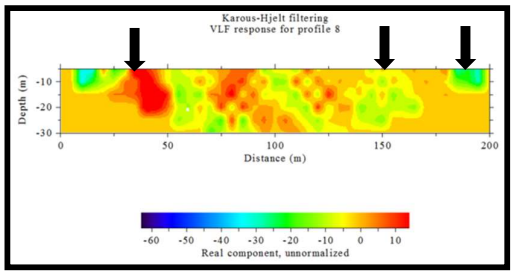

c. 2D cross-section equivalence of VLF response (P8)

Fig.16. VLF-EM Responses for profile 8

The cross-section of the apparent current density of profile 12 (Fig. 17a) reveals the presence of anomalies between 5 – 20 m (top location, 10 m), 60 – 65 m (top location, 70 m), 80 m – 100 m (top location, 85 m), and 115 m – 125 m (top location, 120 m). Figure 17b shows the Fraser filtering Plot for profile 12 In-phases VLF responses generated using the *KH-Filter* Geophysical software program from which figure 17c was produced. The inversion of profile 12 (Fig. 17c) demonstrates the presence of low resistivity values below 15Ωm which extend to 20 m depth; this coincides with the landfill structure boundaries between 25 m to 80 m and from 90 m to 120 m and 130 and 170 m. The cross-section of the apparent current density of profile 16 (Fig. 18a) reveals the presence of anomalies between 140 m – 160 m (top location, 150 m). Figure 18b shows the Fraser filtering Plot for profile 8 In-phases VLF responses generated using the *KH-Filter* Geophysical software program from which figure 18c was produced. The inversion of profile 12 (Fig. 18c) demonstrates the presence of low resistivity values below 15Ωm which extend to 30 m depth; this coincides with the landfill structure boundaries between 25 m to 30 m and from 60 m to 80 m and 110 m and 150 m.

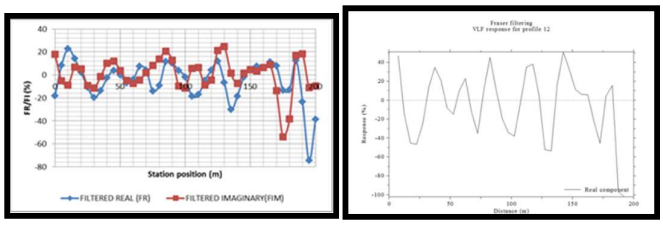

a. Filtered real and filtered imaginary *b. Fraser Filter In-phase plot*

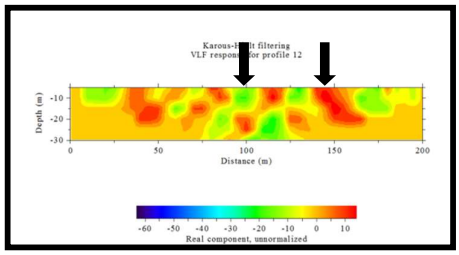

c. 2D cross-section equivalence of VLF response (P12)

Fig.17 VLF-EM Responses for profile 12

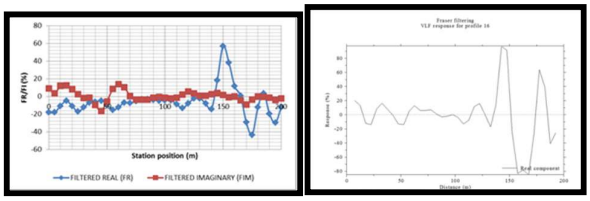

a. Filtered real and filtered imaginary *b. Fraser Filter In-phase plot*

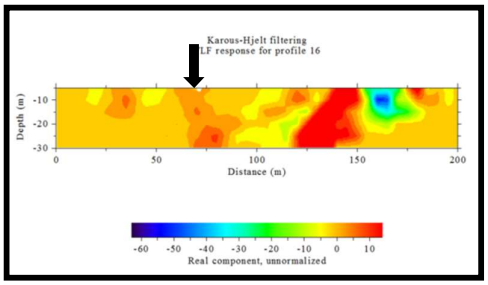

c. 2D cross-section equivalence of VLF response (P16)

Fig.18. VLF-EM Responses for profile 16

3.2 VES Results

Interpretation of VES data shows that the study area is composed of five different Geoelectrical curve types. The field-curve types identified are A, H, Q, K, and KH. The H type constitutes about 44.8%, K which constitutes about 37.9%, and both A and Q type constitutes 6.99%, while the KH curve accounts for about 3.5%. Worthington [35] showed that field curves often mirror image geo-electrically the nature of the successive lithologic sequence in an area and hence can be used qualitatively to assess the groundwater prospect of an area. The H and KH curves which are often associated with groundwater possibilities [36] are pertinent to the study area. The geo-electric sections show subsurface variation in electrical resistivity along the profiles and attempt to correlate the geo-electric sequence across the profiles.

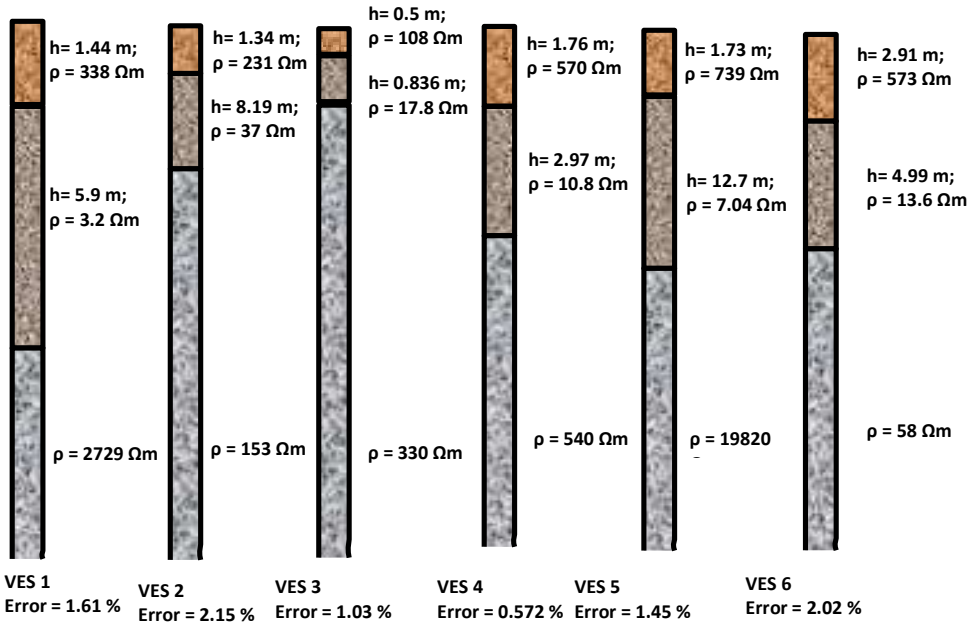

Fig.19. Sample Geo-Electric section showing inferred subsurface lithology for the profiles (VES 1-6)

3.3 Thickness and Resistivity distribution maps

Based on visual examination of the 2-D geo-electric earth parameters; several maps were generated. Figure 20 shows the overburden thickness distribution of the lateritic clay unit which varies from 0.5 m to 6.3 m. Figure 21 shows the aquifer thickness distribution of the main aquifer unit (weathered and fractured layer) which varies from 0.836 m to 58.5 m.

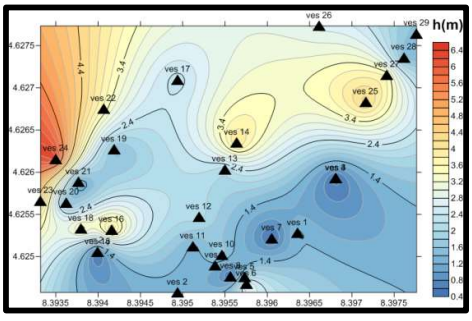

Fig.20. Overburden thickness distributions (CI. 0.5 m)

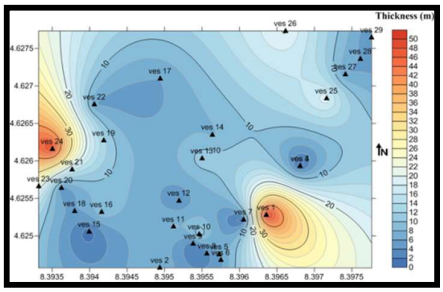

Fig.21. Aquifer thickness distributions (CI. 2.0 m)

The results of geo-electrical surveys were also presented as iso-resistivity maps. Fig. 22 – Fig 24 gave the variation in the resistivity values of the VES points at the topsoil, weathered/fractured rock (aquifer unit), and the basement complex. Figure 22 was produced to determine the resistivity distribution in the subsurface. The resistivity value of the subsurface is highest (> 550 Ωm) in the southeastern and northeastern part (around VES 4, 5, 6, 7, 13, 23, 27, 28, 29). The high resistivity value associated with these parts is possibly due to the permeable nature which aid the distribution of the leachates to the surrounding environment, VES 1 - 3, VES 8 - 12, VES 14 – 22, and VES 24 - 26, have low resistivity in the region of ≤ 500 Ωm. These low values are probably due to the effect of the leachates from the dump site which spread northward and to the southeastern part of the study area. Fig. 23 gave the variation in the resistivity values of the VES points at the aquifer. This was done by contouring the resistivity values acquired at the aquiferous region/zones. The map was produced to distinguish two distinct zone of high and low resistive zone corresponding to unpolluted and contaminated subsurface. The resistivity value of the subsurface is highest (>140 Ωm) in the northwestern and the south eastern part (around VES 4, 7, 11, 14, and 17). The high resistivity value associated with these parts is possibly due to the permeable nature which aid the distribution of the leachates to the surrounding environment, VES 1 - 3, VES 5 - 6, VES 8 – 10, VES 12 – 13, VES 15 – 16 and VES 18 - 29 have low resistivity in the region of ≤100 Ωm. These low values are probably due to the effect of the leachates from the dump site which spread northward. Fig. 24 gave the variation in the resistivity values of the VES points at the basement rock. The resistivity value of the subsurface is highest (>8000 Ωm) in the northeastern and the southeastern part (around VES 5, 8, 13, 25, and 26). VES 1 - 4, VES 6 - 7, VES 9 – 12, VES 14 – 24, and VES 27 – 29 have low resistivity in the region of ≤ 7000 Ωm. With regards to the significant role played by weathered rock thickness in groundwater abstraction (Adiat et al. 2009; Omosuyi et al. 2008), Areas characterized by a thickness between 10.6 –32.8m will be accorded more preference in groundwater development.

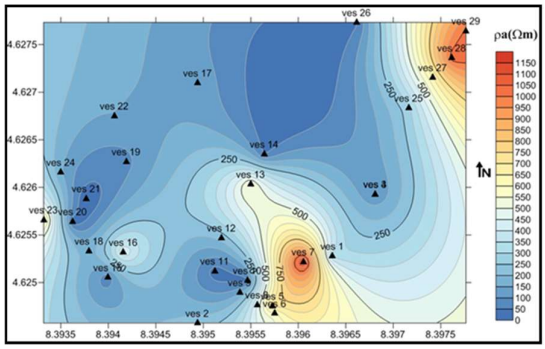

Fig. 22 Overburden resistivity distributions (CI. 50 Ωm)

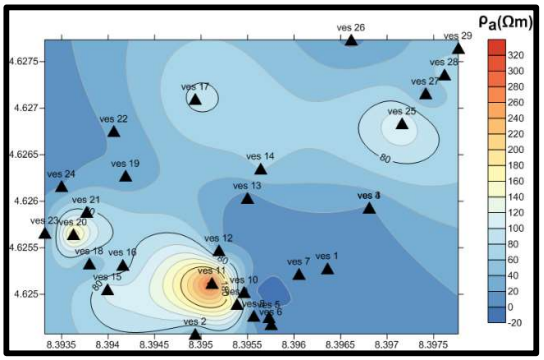

Fig.23. Aquifer resistivity distributions (CI. 20 Ωm)

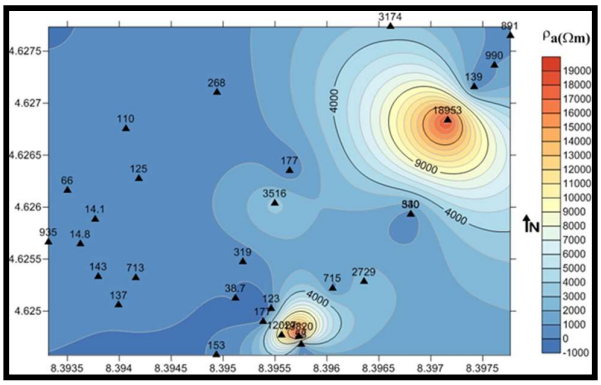

Fig.24 *Basement resistivity variations (CI. 1000 Ωm)*

3.4 3D views of Bedrock and Aquifer

The geophysical software package [37] for VES interpretation generates a set of depth and thickness of layers with the corresponding resistivity values (Table 1). The bedrock depths and the overburden thickness were obtained from these depth estimates. Because overburden is any less compacted material that overlain the bedrock. Therefore, the depth to bedrock is indirect equals to the overburden thickness. The data was then used to produce the bedrock topography map, by picking all depth to bedrock values corresponding to the resistivity values assumed for bedrock for all VES points (Figure 4.23) and the overburden thickness contour map using the Surfer Geophysical software package (Figure 4.18).

In figure 25, it could be seen that the bedrock has an irregular topography which is deeper towards the North – Western and the South – Eastern part with depth (> 30 m) correspondent to VES 1 and 24. The lesser to intermediate depth is (≤ 25 m) towards the Northwestern and southeastern part correspondent to VES 2 - 23, and VES 25 – 29. That is to say, where we have the deepest, intermediate and the shallowest bedrock depth corresponded to thickest, intermediate, and the thinnest overburden thickness respectively.

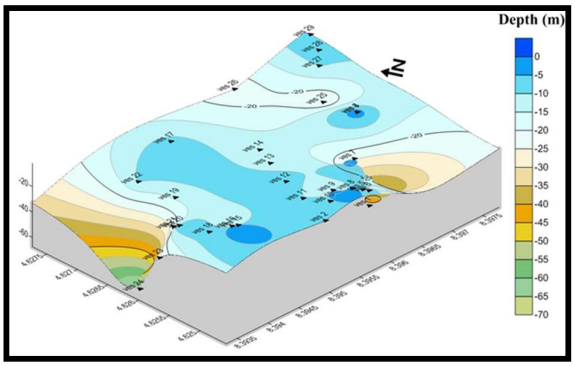

Fig.25 3D view of the Bedrock Topography

Table 1. Summary of aquifer parameters

VES NO	Aquifer Depth (m)	Aquifer thickness (m)	Lithology	Aquiferous Layer number
1	1.44	5.9+	Weathered, Basement	2nd
2	1.34	8.19+	Weathered and Fractured Basement	2nd and 3rd
3	0.5	0.836	Weathered and Fractured Basement	2nd and 3rd Layer
4	1.76	2.97+	Weathered and Fractured Basement	2nd and 3rd Layer
5	1.73	7.04	Weathered Basement	2nd Layer
6	2.91	4.99+	Weathered and Fractured Basement	2nd and 3rd Layer
7	0.5	0.836+	Weathered and Fractured Basement	2nd and 3rd Layer
8	0.5	3.11	Weathered Basement	2nd Layer
9	1.34	2.23+	Weathered and Fractured	2nd and 3rd Layer

			Basement	
10	7.23	11.8+	Weathered and Fractured Basement	3rd and 4th Layer
11	1.34	8.36+	Weathered and Fractured Basement	2nd and 3rd Layer
12	2.1	4.17+	Weathered and Fractured Basement	2nd and 3rd Layer
13	2.06	11.4	Weathered Basement	2nd Layer
14	6.04	7.74+	Weathered and Fractured Basement	2nd and 3rd Layer
15	0.5	0.836+	Weathered and Fractured Basement	2nd and 3rd Layer
16	4.06	9.62	Weathered Basement	2nd Layer
17	2.28	6.01+	Weathered and Fractured Basement	2nd and 3rd Layer
18	3.57	5.96+	Weathered and Fractured Basement	2nd and 3rd Layer
19	1.55	13 +	Weathered and Fractured Basement	2nd and 3rd Layer
20	1.55	4.58+	Weathered and Fractured Basement	2nd and 3rd Layer
21	1.18	16.4+	Weathered and Fractured Basement	2nd and 3rd Layer
22	3.57	5.96+	Weathered and Fractured Basement	2nd and 3rd Layer
23	4.25	21.6	Weathered Basement	2nd Layer
24	9.53	5.85+	Weathered and Fractured Basement	2nd and 3rd Layer
25	5.96	19.4	Weathered Basement	2nd Layer
26	2.72	20.4	Weathered Basement	2nd Layer
27	3.57	6+	Weathered and Fractured Basement	2nd and 3rd Layer
28	1.45	5.93	Weathered Basement	2nd Layer

29	1.52	4.5+	Weathered and Fractured Basement	2nd and 3rd Layer

Figure 26 also show irregular water table topography with a depth range of 0.5 m to 9.53 m. The deeper water table depth (7 m to 9.53 m), corresponded to VES 10 and VES 24 which is located towards the Northwestern part of the study area, and the shallow aquifer running from depth of 0.5 m.

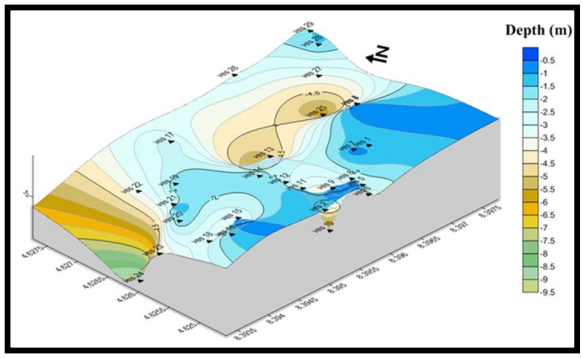

Fig.26. 3D view of the top of Aquifer

4. DISCUSSION

The conductivity and resistivity properties of near-surface rocks and soil around a reclaimed dumpsite were investigated using VLF-EM and Electrical Resistivity Surveys. This analysis aims to map the leachate plume in the region to see if there has been any leachate penetration into shallow aquifers. It is evident that the leachate has penetrated in the N-S and E-W direction. The study's goals include assessing the extent of leachate penetration, fracture distribution, geo-electric layer number, and depth to fresh basement rocks.

The VLF-EM data models depict the contamination plumes inside the waste disposal site as conductive anomalies while the geo-electric sections of the VES detected the contaminated zones at the subsurface as resistive anomalies. The resistivity values obtained from ER coring inside the reclaimed dumpsite are significantly lower than those obtained outside the reclaimed dumpsite. The analysis of the geo-electric sections generated revealed that the zone with leachate pollution (the second geo-electric layer) has thicknesses ranging from 0.5 m to 6.3 m and a maximum depth of 9.53 m to the basement and the depth of the hand dug wells in the research area varied between 4.1 m and 5.5m showing that most of the wells there terminate within the contaminated zone. This observation indicates that the leachate plumes have actually extended to a depth of 9.53 m at the subsurface. The infiltration of contamination plumes was due to the high porosity and

permeability characteristics of the soil type present in the research area. Remediation of leachate contamination in the area can be achieved by either pump–and–treat technique or co-treatment technique. This study also reveals the importance of using an integrated approach of geophysical techniques for acquiring the physical properties of a waste disposal site. The employment of different techniques allows the resolution of possible discrepancies and reveals the most accurate description of a waste disposal site's characteristics.

4.1 Correlation

There are strong agreements in the results of VLF-EM and VES, - indicating the presence of leachate at depth below the overburden. Compared to the area outside the dumpsite, the resistivity values obtained from the VES around the reclaimed dumpsite are far lower than the resistivity values obtained outside the dumpsite. Similarly, the current density value obtained around the reclaimed dumpsite by the VLF-EM study is far higher than those obtained outside the dumpsite. The highest positive current density recorded outside the dumpsite is about 5.0% while the highest recorded around the reclaimed dumpsite is about 10.0 %. From these, we also conclude that the presence of leachate raised the conductivity, or reduced the resistivity of the soil and rocks around the dumpsite. This study is important for groundwater exploration and groundwater quality control in the area. Groundwater in the depth range of 20 m in the study area is not safe for drinking except when treated. Remediation of leachate contamination in the area can be achieved by either pump–and–treat technique or co-treatment technique.

The correlation of these investigations with [34], [38] physio-chemical work and bio-chemical and histological work on the dumpsite shows a strong correlation with the results of the VLF – EM, and VES carried out on the dumpsite.

5. CONCLUSION

In conclusion:

i. Leachate contamination is still present in the area after some years of abandonment of the dumpsite due to a cholera outbreak and removal of the waste materials to a permanent site at Eiyenkorin.

ii. The overburden thickness could not prevent the leachate from intruding shallow aquifers due to the thickness ranges between 0.5 m and 6.3 m in which only the northwestern part of the area that has thick overburden.

iii. The correlation of these investigations with (Mokuolu et al., 2017; and Musa and Sikemi, 2020) physio-chemical work and bio-chemical and histological work on the dumpsite shows a strong correlation with the results of the VLF – EM, and VES carried out on the dumpsite.

ACKNOWLEDGEMENTS

The authors acknowledge the supports of the University in carrying out this research.

DECLARATIONS

Funding: This research did not receive any specific grant from funding agencies in the public, commercial, or not-for-profit sectors

Conflicts of Interest/Competing interest: The author has no declarations to make

REFERENCES

[1] Diersing W, Nancy F:"Water Quality: Frequently Asked Questions". PDA. N. O. A. A. http://floridakeys.noaa.gov/pdfs/wqfaq.pdf. Retrieved; 2009-08-24

[2] Sunmonu L.A, Olafisoye, E.R, Adagunodo, T.A, Ojoawo. I.A. and Oladejo, O.P. Integrated Geophysical Survey In A Refuse Dumpsite Of Aarada, Ogbomoso, and Southwestern-Nigeria. IOSR Journal of Applied Physics (IOSR-JAP) ISSN: 2278-4861.Volume 2, Issue 5(Nov. -Dec. 2012), PP 11-20www.iosrjournals.org

[3] Ramakrishnaiah CR, Sadashivaiah C, Ranganna G. Assessment of water quality index for groundwater in Tumkur Taluk, Kamataka state, India. E J Chem 6(2):523–530

[4] Rizwan R, Gurdeep S. Assessment of groundwater quality status by using water quality index method in Orissa, India.World Appl Sci J 9(12):1392–1397

[5] Ganiyu, S.A, Badmus, B.S, Oladunjoye, M.A, Aizebeokhai, A.P, Ozebo V.C, Idowu, O.A, and Olurin, O.T. Assessment of groundwater contamination around active dumpsite in Ibadan southwestern Nigeria using integrated electrical resistivity and hydrochemical methods. Environ Earth Sci (2016) 75:643. https://doi.org/10.1007/s12665-016-5463-2

[6] Raji, W.O, and Adeoye., T.O. Geophysical mapping of contaminant leachate around a reclaimed open dumpsite. Journal of King Saud University – Science (2017)29, 348–359. https://dx.doi.org/10.1016/j.jksus.2016.09.005

[7] MacDonald, A.M., Bonsor, H.C., Dochartaigh, B.E.O., Taylor, R.G. A quantitative map of groundwater resource in Africa. Environ. Res. Lett. 7, 024009

[8] Karlik, G., Kaya, A. Investigation of groundwater contamination using electric and electromagnetic methods at an open waste-disposal site: a case study from Isparta, Turkey. Environ. Geol. 40(6), 34–42

[9] Ulrych, T.J, LimA, O.A, Sampaio, E.E. Search of plumes: a GPR odyssey in Brazil. In: The 64th annual international met. Society exploration geophysical SEG, Los Angeles, USA, 569-572

[10] Jemmi. L, Muller. R, Green. A, Pugin. A, Huggenberger. P. Integrated studies of Swiss waste disposal sites: results from geo-radar and other geophysical surveys. In: The 5th international conference on ground penetrating radar (GPR '94). Kitchener, Ontario, pp 1261–1274

[11] Atekwana, E.A, Sauck, W.A., Werkema, D.D. Investigation of geo-electrical signatures at a hydrocarbon-contaminated site. J. Appl. Geophys. 44:167-180

[12] Orlando. L and Marchesi. E. Geo-radar as a tool to identify and characterize solid waste dumps deposits. J. Appl. Geophys. 48:168-174

[13] Stanton, G.P., and Schrader, T.P. Surface geophysical investigation of a chemical-waste landfill in northwestern Arkansas. U.S. Geological Survey Karst Interest Group Proceedings. Kuniansky EL (Ed.), Water-Resources Investigations Report 01-4011, pp.107–115.

[14] Carpenter, P.J., Calkin, S.F., Kaufmann, R.S. Assessing a fractured landfill cover using electrical resistivity and seismic refraction techniques. Geophysics 56 (11), 1896–1904

[15] Carpenter, P.J., Calkin, S.F., Kaufmann, R.S. Assessing a fractured landfill cover using electrical resistivity and seismic refraction techniques. Geophysics 56 (11), 1896–1904

[16] Powers, C.J., Wilson, J., Haeni, F.P., Johnson, C.D. Surface geophysical investigation of University of Connecticut Landfill, Water Resources Investigations Report 99- 4211. U.S. Department of the Interior U.S. Geological Survey

[17] Porsani, L., Filho, W.M., Ellis, V.R., Shimlis, J.D., Moura, H.P. The use of GRR & VES in delineating contamination plume in a landfill site. A case study in SE Brazil. J. Appl. Geophys. 155, 199–209.

[18] Bernstone, C., Dahlin, T., Ohlsson, T., Hogland, W. DC-resistivity mapping of internal landfill structure: two pre-excavation surveys. Environ. Geol. 39, 3–4.

[19] Dobrin, M.B. Introduction to Geophysical prospecting. McGraw-Hill Company, New York.

[20] Zohdy, A.A.R. A new method for the automatic interpretation of Schlumberger and Wenner sounding curves. Geophysics 54 (2), 245–253. https://dx.doi.org/10.1190/1.1442648.

[21] Santos, M.F.A., Mateus, A., Figueiras, J., Gonclaves, M.A. Mapping groundwater contamination around a landfill facility using VLF-EM method – a case study. J. Appl. Geophys. 60, 115–125

[22] Ajadi B.S., Adaramola, M.A., Adeniyi, A., and Abubakar, M.I. Effects of effluent discharge on Public Health in Ilorin metropolis, Nigeria. Ethiopian Journal of Environmental Studies & Management 9(4): 389 – 404, 2016. ISSN: 1998-0507. DOI: https://dx.doi.org/10.4314/ejesm.v9i4.1

[23] Oyegun, R.O. Water Resources in Kwara State. Matanmi and Sons Printing and Publishing Co. Ltd. Ilorin, pp: 113

[24] Rahaman MA. Review of the basement geology of South-Western Nigeria. In: Kogbe CA(ed) Geology of Nigeria, 2nd edn., Elizabethan Publishers, Lagos, pp 41–58

[25] Obaje N. G. Geology and Mineral Resources of Nigeria. ISSN 0930-0317ISBN 978-3-540-92684-9e-ISBN 978-3-540-92685-6DOI 10.1007/978-3-540-92685-6

[26] Karous M, and Hjelt SE. Linear filtering of VLF dip-angle measurements. Geophysical Prospecting. 1983;(31):782–794

[27] Sinha, A.K. Interpretation of ground VLF-EM data in terms of vertical conductor models. Mineral Resources Division, Geological Survey of Canada, 601 Booth St., Ottawa, Ont. K1A 0E8 Canada. https://doi.org/10.1016/0016-7142(90)90005-D

[28] Karkkonen, P. and Sharma, S.P. Delineation of near surface structures using VLF-EM and VLF-R data: insight from the joint inversion results. Leading Edge Vol. 16: 1683-1686

[29] McNeill, J.D., Labson, V. Geological mapping using VLF radiofields electromagnetic methods. In: Nabighian, M.N. (Ed.), . In:Applied Geophysics, vol. 2. SEG, Tulsa, OK, pp. 521–640

[30] Pirttijarvi, M. Karous-Hjelt and Fraiser Filtering of VLF Measurements. KHFFILT Users' Guide (2004).

[31] Koefoed, O. Geo-sounding Principles, 1 – Resistivity Sounding Measurements. Elsevier, Amsterdam (1979)

[32] Orelana, E.A., Mooney, H.M. Master Tables and Curves forVertical Electrical Sounding over Layered Structures. Intergencia,Madrid, p. 159

[33] Alex, A.B., Igor, N.M., Vladimir, A.S.. Authomated and Semi-authomated Interpretation of Vertical Electrical Sounding and Induced Polarization Data obtained from A Variety of Popular Arrays used in Electrical Prospecting, IPI2Wi. Geological and Geophysical Department, Moscow State University

[34] Musa, T.Y and Sikemi, A.O. Impact of groundwater samples and leachates from Gbagede dumpsite, Amoyo, Kwara State, Nigeria, on testes and prostate of male Wistar rats: A biochemical and histological study. DOI: 10.1111/and.13801

[35] Worthington PF. Influence of matrix conduction upon hydro geophysical relationships in arenaceous aquifers. Water Resour. Res 13(1):87–92

[36] Omosuyi GO, Adeyemo A, Adegoke AO. Investigation of Groundwater Prospect using Electromagnetic and Geoelectric Sounding at Afunbiowo, near Akure, Southwestern Nigeria

[37] Bobachev, C. "IPI2Win: A Windows Software for an Automatic Interpretation of Resistivity Sounding Data," PhD Thesis, Moscow State University, Russia, 2002.

[38] Mokuolu, O.A., Jacob, S.O., Ayanshola, A.M. Groundwater quality assessment near a Nigerian dumpsite. Ethiopian Journal of Environmental Studies & Management 10(5): 588 – 596, 2017. ISSN:1998-0507. DOI: https://dx.doi.org/10.4314/ejesm.v10i5.3

How to cite this article:
Olatunji S, Fauzan A. Geophysical assessment of groundwater contaminations from leachate intrusion in amoyo dumpsite. J. Fundam. Appl. Sci., 2022, *14(1), 181-209.*